

# Comparison of Output Parameters of Two-Phase Interleaved Buck Converter Using Different Type Control Methods

Hilmi ZENK

Department of Electrical-Electronics Engineering  
Engineering Faculty, Giresun University  
Giresun, Turkey  
hilmi.zenk@giresun.edu.tr

**Abstract**—Electrical power converters are widely used in electrical and electronics area. In this study, the continuous conduction mode of the interleaved buck converter; the unit power factor (UPF) and the total harmonic distortion (THD) of the input current are investigated using proportional-integral (PI) control and average sliding mode control (ASMC). The Buck Converter simulates MATLAB / Simulink at 1kW power and 20 kHz switching frequency and analyzes the control methods. In the analyzes, the THD effect of the converter's response to the load changes in the control methods and other parameter changes was investigated.

**Keywords**—interleaved buck converter; proportional-integral (PI) control; average sliding mode control (ASMC); unit power factor (UPF); total harmonic distortion (THD).

## I. INTRODUCTION

The widespread use of semiconductor switches has accelerated the pace of development of the technology, which has brought with it some electrical problems. At the beginning of these problems, the harmonics in the electricity distribution system increase, and the sinusoidal current waveform deteriorates. Many researchers are working on different types of circuit designs to reduce the harmonics in the currents feeding the systems that contain the power switches.

The power sources used in power electronic converters draw non-sinusoidal and harmonic currents from the network. These currents drawn from the system cause low power factor (PF) and high line currents to be generated. Decreasing the quality of the current drawn from the network; Resulting in deterioration of the mains voltage, increased losses, the emergence of electromagnetic parasites and inefficient use of consumed power [1]. Many researchers are working on different types of circuit designs to meet the electrical quality standards introduced by some international organizations and to improve the power coefficient. Based on these standards, using passive circuits, techniques such as reducing harmonic components, correcting active power coefficient and active rectifiers are used to derive electrical adverse effects [2]. There are different

circuit topologies of power converters for correcting the power factor such as buck, boost, flyback, interleaved structure [3-7].

Most DC/DC converters are usually provided a low output voltage and high output current to load. Therefore, a conventional interleaved buck converter (IBC) as shown in Figure 1 is widely adopted, because it has a simple structure, high output current density and low output current ripple. However, in high step-down voltage applications, it suffers from extremely short duty ratio and high component stresses, resulting in low conversion efficiency [8-11].

## II. INTERLEAVED BUCK CONVERTER

The circuit diagram of IBC is given as shown in Figure 1. This is equivalent to a parallel combination of two sets of switches, diodes and inductors connected to a common filter capacitor and load [12]. The switches are operated out of phase. Assume the converter operates with duty ratio less than 50% and in continuous conduction mode [13].

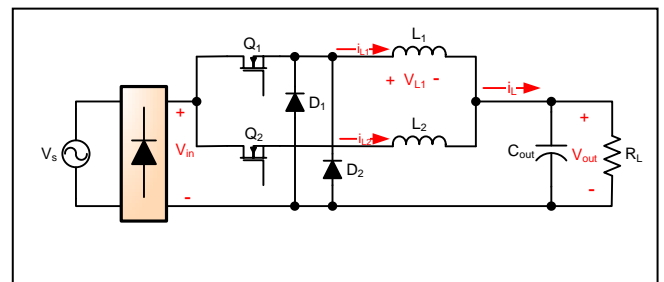


Fig. 1. Simple circuit diagram of 2 phase IBC

A two phase IBC will operate in four different modes and is explained as follows.

### A. IBC Mode-1

In Operation mode-1 switch  $Q_1$  is turned on by giving a gate pulse. At the same time switch  $Q_2$  is off. Current flows through the switch  $Q_1$ , inductor  $L_1$  and load, making current through  $L_1$  to increase as long as  $Q_1$  is turned on. During this time current in  $L_2$  decreases linearly. The equivalent circuit is as in Figure 2. The variations of  $i_{L1}$  and  $i_{L2}$  during  $T$  are given by,

$$\Delta i_{L1} = \left( \frac{V_{in} + V_{out}}{L_1} \right) T_1 \quad (1)$$

$$\Delta i_{L2} = \left( \frac{-V_{out}}{L_2} \right) T_1 \quad (2)$$

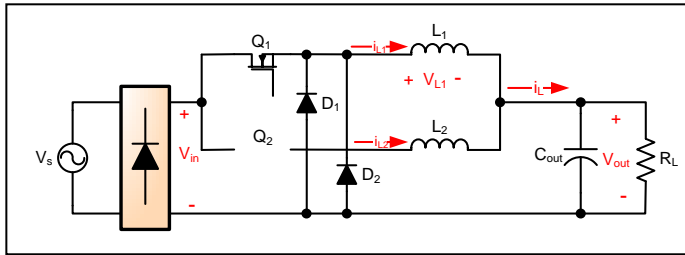


Fig. 2. Equivalent Circuit of IBC in Mode 1

**B. IBC Mode-2**

Since IBC operates with a duty cycle less than 0.5, in this mode both the switches are OFF. Diodes D<sub>1</sub> and D<sub>2</sub> are the conducting devices. The equivalent circuit is illustrated in Figure 3. The energies stored in L<sub>1</sub> and L<sub>2</sub> are released to the load through the forward biased diodes. So i<sub>L1</sub> and i<sub>L2</sub> are decreased linearly. Thus the variations in i<sub>L1</sub> and i<sub>L2</sub> during T<sub>2</sub> are given by,

$$\Delta i_{L1} = \left( \frac{-V_{out}}{L_1} \right) T_2 \quad (3)$$

$$\Delta i_{L2} = \left( \frac{-V_{out}}{L_2} \right) T_2 \quad (4)$$

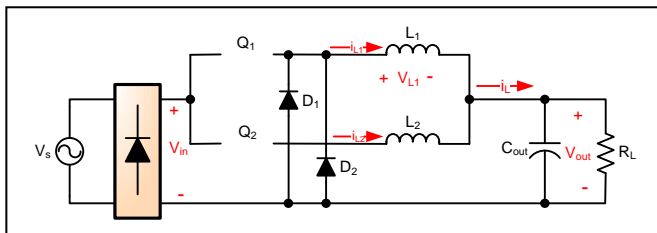


Fig. 3. Equivalent Circuit of IBC in Mode 2

**C. IBC Mode-3**

During T<sub>3</sub> Q<sub>2</sub> is turned On and Q<sub>1</sub> turned off. The equivalent circuit is illustrated in Figure 4. The turning on of Q<sub>2</sub> charges the inductor L<sub>2</sub> and since Q<sub>1</sub> is off inductor L<sub>1</sub> is discharged to the load. The variations in i<sub>L1</sub> and i<sub>L2</sub> during T<sub>3</sub> are given by,

$$\Delta i_{L1} = \left( \frac{-V_{out}}{L_1} \right) T_3 \quad (5)$$

$$\Delta i_{L2} = \left( \frac{V_{in} - V_{out}}{L_2} \right) T_3 \quad (6)$$

Equation (5) shows i<sub>L1</sub> linearly decreasing during T<sub>3</sub> since the slope is negative and a constant.

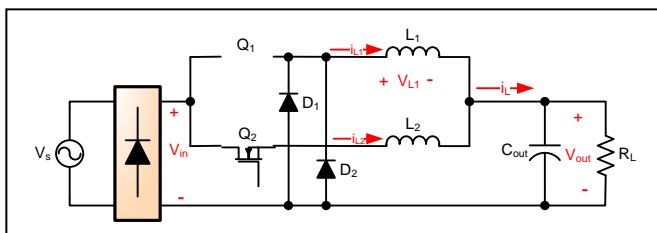


Fig. 4. Equivalent Circuit of IBC in Mode 3

**D. IBC Mode-4**

The operating mode is same as mode 2. The variations in i<sub>L1</sub> and i<sub>L2</sub> during T<sub>4</sub> are given as in equation (3) and (4).

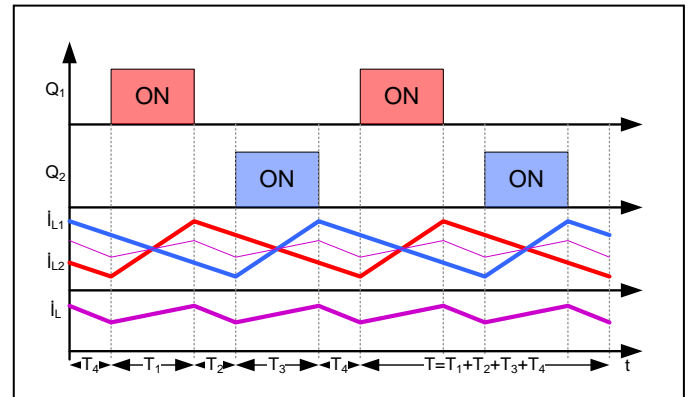


Fig. 5. Inductor Current Waveforms

**III. SYSTEM CONTROL LOOP**

The converter is controlled with a voltage mode control scheme. The PWM module is configured for IBC mode with an independent time-base. The DC Link voltage is measured by the voltage sensors and sent to DSP control. This value is subtracted from the voltage reference in software to obtain the voltage error. The voltage error is then fed into a control algorithm that produces a duty cycle value based on the voltage error, previous error, and control history. The output of the control algorithm is also clamped to minimum and maximum duty cycle values for hardware protection. The voltage mode control algorithm must be executed at a fast rate in order to achieve the best transient response. Therefore, the control algorithm is executed in the ADC interrupt service routine, which is also assigned the highest priority in the UPS code. A block diagram of the push-pull converter control scheme is shown in Figure 6.

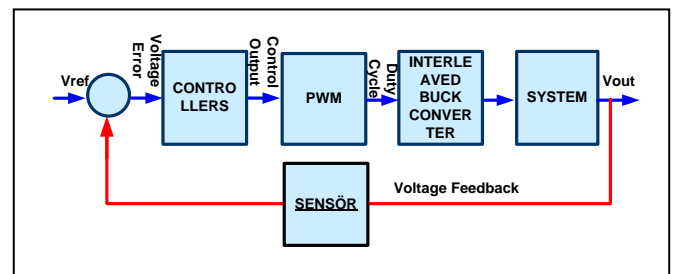


Fig. 6. A Block diagram of IBC voltage control loop

**IV. CONTROL SYSTEMS MODELS**

The only difference in control methods for interleaved converters is the number of feedback cycles. For the N-phase converter, there is N number of feedback cycles. Additional circuitry is needed to enable phase shift operation in the interleaved loop. Hence, all control techniques are designed according to single phase and D duty ratio is shifted by phase difference. This section describes control methods that synchronize the input current with the basic component of the input voltage [14].

A. Proportional Integral (PI) Control

Proportional-integral (PI) controller is one of the commonly used techniques to correct the power factor. In this method, the average inductor current is taken and this average value is controlled by switching.

$$I_{ref} = [(V_{ref} - V_{out})V_{EAV}]V_{in} \quad (7)$$

$$D = D_1 = (I_{ref} - |I_{in}|)V_{EAI} \quad (8)$$

$$V_{EAV} = \left( K_{pv} + \frac{K_{iv}}{s} \right) \quad (9)$$

$$V_{EAI} = \left( K_{pi} + \frac{K_{ii}}{s} \right) \quad (10)$$

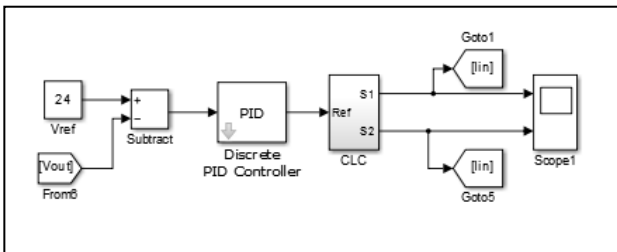


Fig. 7. PI controller block for Simulink Model of IBC

In equations,  $V_{EAV}$ , Proportional-integral controlled voltage error amplifier,  $V_{EAI}$ , Proportional-integral controlled current error amplifier,  $D$ , duty cycle. In the proportional-integral controller,  $K_p$  and  $K_i$  can be selected according to the method of Ziegler-Nichols. The PI control method follows the actual current reference to provide a unit power factor and low THD [14]. Figure 7 shows the proportional integral control method.

B. Average Sliding Control Method

Control of systems with nonlinear and complex dynamics is very difficult with classical supervisory methods. The Average Sliding Control Method (ASCM) can be an effective control method in the control of such systems. The purpose of applying the ASCM method to closed-loop control systems is to push the error to the sliding surface or, alternatively, to the switching surface and keep it at that surface.

Since the slip surface is defined as a function which is a linear combination of state variables, the state variables are linearly dependent on this surface. In this case, the system is reduced to a level independent input variable, and the system is controlled by a reduced control rule [15].

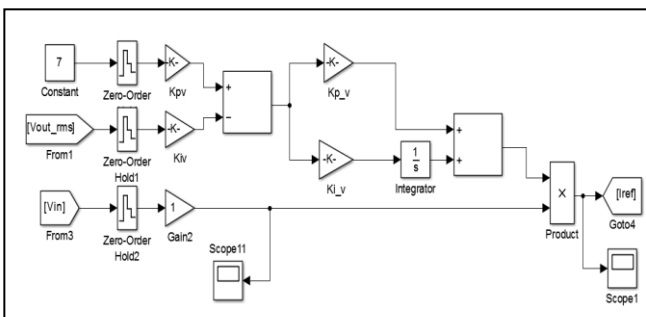


Fig. 8. Voltage controller block for Simulink Model of IBC

The voltage controller has the same structure as shown in Figure 8 according to all control methods. Figure 9 shows the average sliding mode control method.

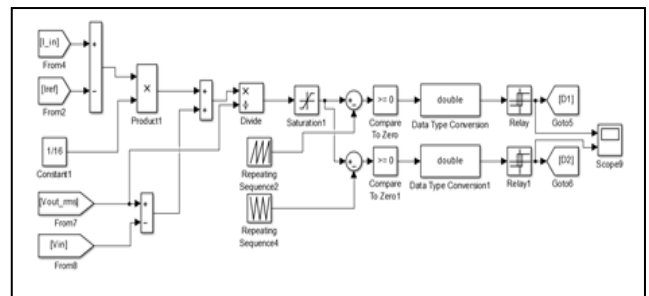


Fig. 9. Average sliding current controller for Simulink Model of IBC

V. SIMULATION OF THE FULL SYSTEM

Simulation studies were performed using the MATLAB / Simulink program. Selected parameters in simulation studies are given in Table 1. The two-cell interleaved buck converter is shown in Figure 10.

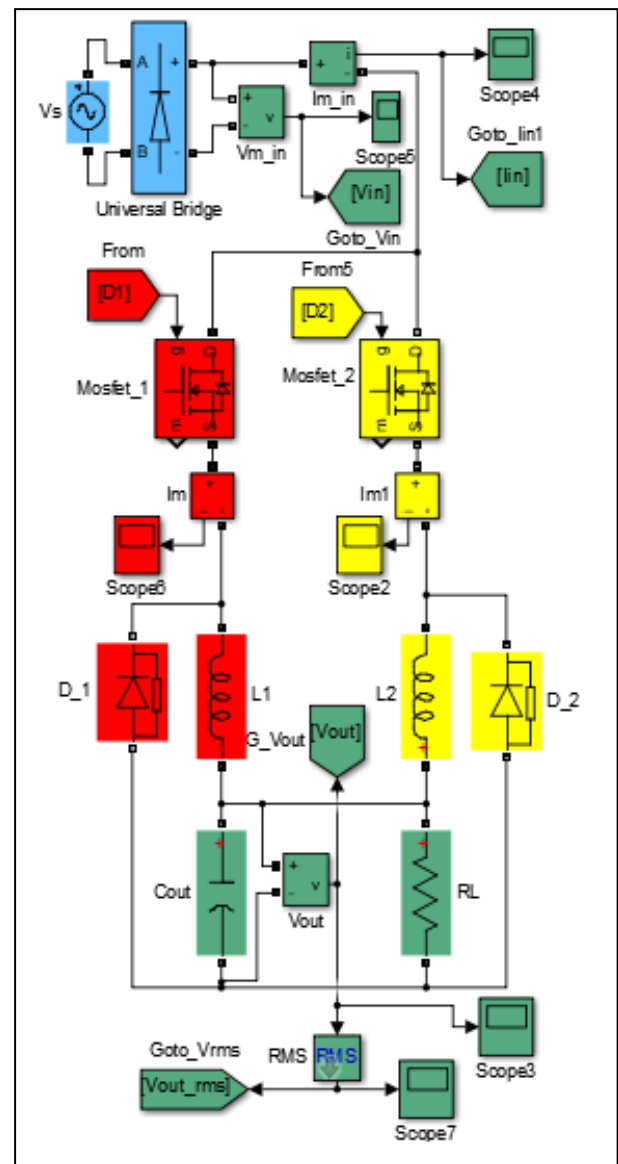


Fig. 10. Simulink Model of IBC

TABLE I. IBC SIMULATION PARAMETERS

Parameters	Symbol	Value
Number of Phases	$N_{\text{phase}}$	2
Input Voltage	$V_{\text{in}}$	150 - 200 V
Output Voltage	$V_{\text{out}}$	24 V
Switching Frequency	F	65 kHz
Per phase Ripple current	$\Delta I$	%10
Output Current	$I_{\text{out}}$	5A
Indutors per phase	$L_1, L_2$	100 $\mu\text{H}$
Output voltage ripple	$V_{\text{o\_ripple}}$	$\leq 20$ mV
Output Capacitor	$C_{\text{out}}$	22 $\mu\text{F}$

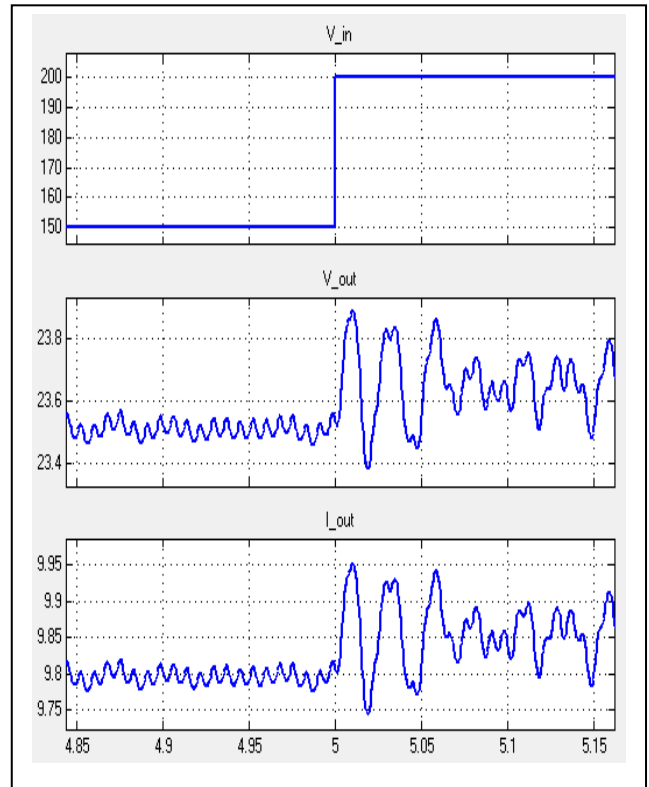


Fig. 12. In PI-controlled IBC, input voltage  $V_{\text{in}}$ , output voltage  $V_{\text{out}}$  and output current  $I_{\text{out}}$  detailed analysis in 5ms

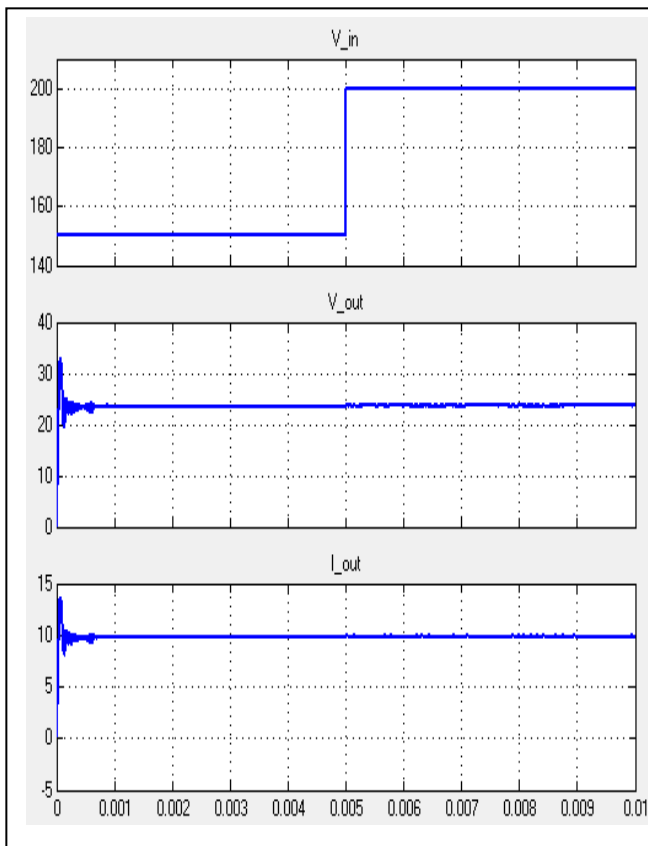


Fig. 11. In PI-controlled IBC, input voltage  $V_{\text{in}}$ , output voltage  $V_{\text{out}}$  and output current  $I_{\text{out}}$

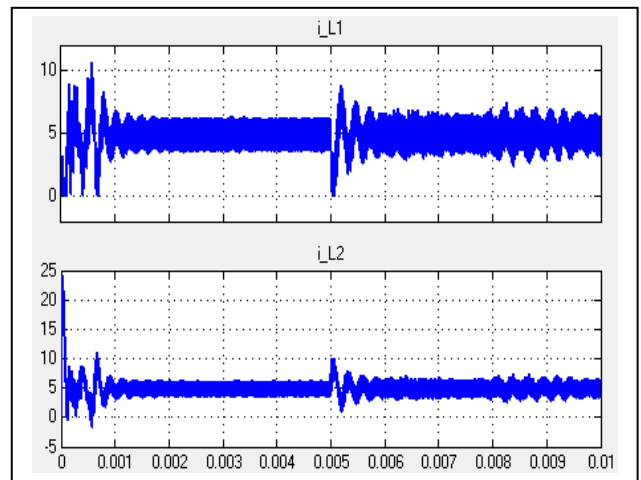


Fig. 13. Change in inductance currents of  $L_1$  and  $L_2$

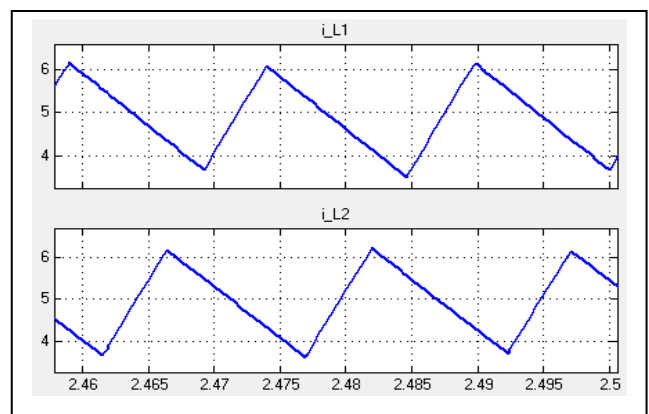


Fig. 14. Detailed analysis of changes in currents of  $L_1$  and  $L_2$

TABLE II. SIMULATION RESULTS

Simulations	1	2	3	4	5	6	7	8
Power (kW)	1	1	1	1	0,5	1	1	1
$L_1=L_2$ (mH)	100	100	100	100	80	50	50	50
$C_{out}$ ( $\mu$ F)	22	22	22	22	22	22	22	22
$V_{out}$ (rms)	200	100	250	220	200	200	150	100
Proportional-Integral Control Method								
Power Factor (PF)	0,99	0,99	0,99	0,99	0,99	0,99	0,99	0,99
THD (%)	5,1	2,0	6,3	4,7	5,2	23,1	8,5	4,5
Average Sliding Control Method								
Power Factor (PF)	0,99	1	0,99	0,99	0,99	0,99	0,99	0,99
THD (%)	4,8	1,4	5,4	3,9	4,2	15,2	6,3	3,9

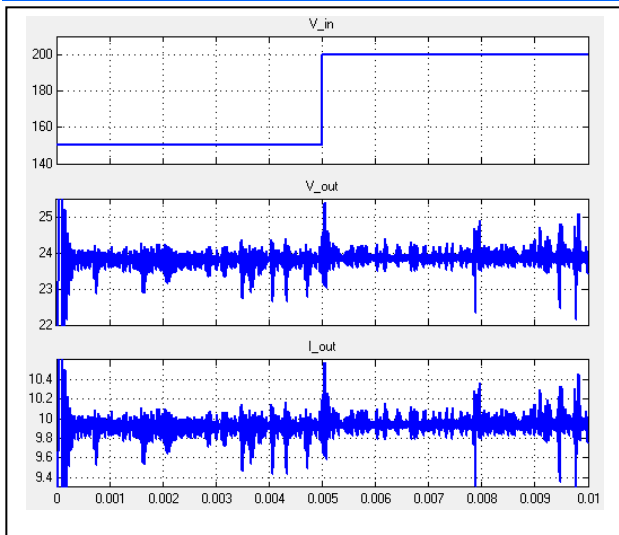


Fig. 15. In ASMC- controlled IBC, input voltage  $V_{in}$ , output voltage  $V_{out}$  and output current  $I_{out}$

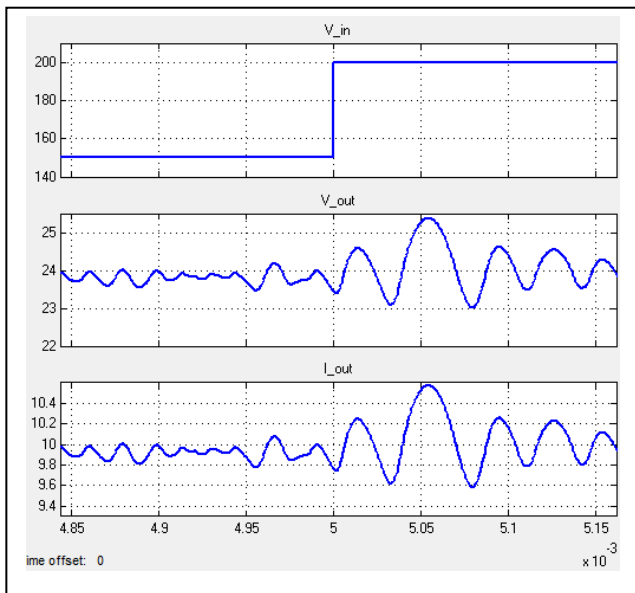


Fig. 16. In ASMC- controlled IBC, input voltage  $V_{in}$ , output voltage  $V_{out}$  and output current  $I_{out}$  detailed analysis in 5ms

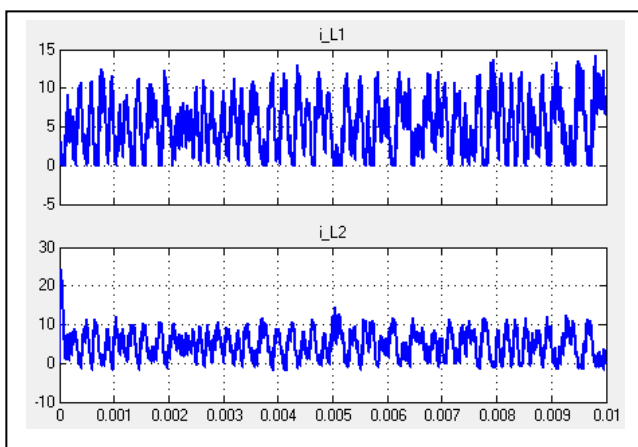


Fig. 17. Change in inductance currents of  $L_1$  and  $L_2$

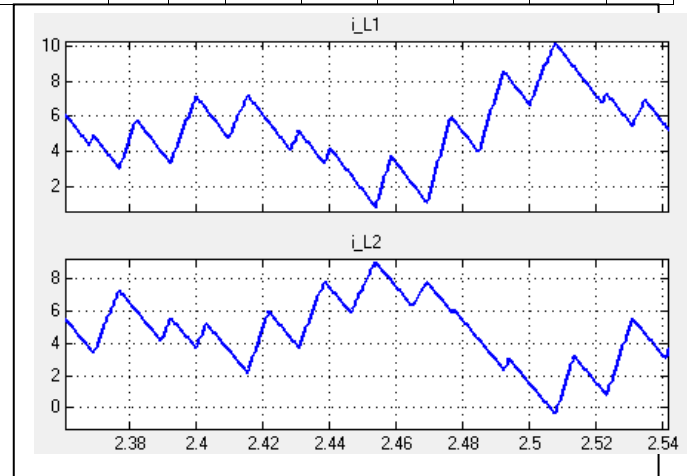


Fig. 18. Detailed analysis of changes in currents of  $L_1$  and  $L_2$

## VI. CONCLUSION

In this study, proportional-integral and average sliding mode network current control methods are applied to a two-cell buck-type power factor correcting circuit and simulated in Matlab / Simulink program. The results obtained are very close to each other. The control techniques used have been based on practical work using fixed switching frequency. It has been

observed that both of the tested control techniques exhibit a structure resistant to output load changes, as can be seen from the graphs. It has been observed that the proportional-integral control technique in the designed 100W simulation circuit is more sensitive to inductor variations than the average floating mode control technique. It has been observed that when the inductor value is reduced, the proportional-integral controller coefficient adjustments must be made again and the average sliding mode method maintains its performance. Capacitor change affects output voltage fluctuation.

#### REFERENCES

- [1] F. Karık, "Ortalama Kayan Kip Metodu ile Denetlenen İki Fazlı Sarmaşık Yapılı Yükseltici Tip Dönüştürücünün Performans Analizi," *Elektrik, Elektronik, Bilgisayar, Biyomedikal Mühendisliği Bilimsel Dergisi*, vol.2, no.4, 2012.
- [2] Z. Chen, B.R. Raymond, and C.L. Fred, "Design Analysis of a Hysteresis Boost Power Factor Correction Circuit," *Power Electronics Specialists Conference PESC '90 Record-21st Annual IEEE*, pp.800-807, 1990.
- [3] C. Qiao, and K.M. Smedley, "A topology survey of single-stage power factor corrector with a boost type input-current-shaper," *IEEE Transactions on Power Electronics*, vol.16, no.3, pp.360–368, 2001.
- [4] L. Po-Wa, L. Yim-Shu, D.K.W. Cheng, and L. Xiu-Cheng, "Steady-state analysis of an interleaved converter with coupled inductors," *Industrial Electronics IEEE Transactions*, vol.47, no.4, pp.787-795, 2000.
- [5] H. Yao-Ching, H. Te-Chin, and Y. Hau-Chen, "An Interleaved Boost Converter with Zero-Voltage Transition," *IEEE Transactions on Power Electronics*, vol.24, no.4, pp.973-978, 2009.
- [6] J.M. Alonso, M.A. Dalla Costa, and C. Ordiz, "Integrated Buck-Flyback Converter as a High-Power-Factor Off-Line Power Supply," *Industrial Electronics IEEE Transactions*, vol.55, no.3, pp.1090-1100, 2008.
- [7] Z.Jun, D.D.C. Lu, and S.Ting, "Flyback-Based Single-Stage Power-Factor-Correction Scheme with Time-Multiplexing Control," *Industrial Electronics IEEE Transactions*, vol.57, no.3, pp.1041-1049, 2010.
- [8] V. Agarwal, R.K. Aggarwal, P. Patidar, and C. Patki, "A novel scheme for rapid tracking of maximum power point in wind energy generation systems," *IEEE Trans. Power Electron.*, vol.25, pp.228–236, 2010.
- [9] P. Wong, P. Xu, and F.C. Lee, "Performance improvements of interleaving VRMs with coupling inductors," *IEEE Trans. Power Electron.*, vol.16, pp.499–507, 2001.
- [10] Y.M. Chen, S.Y. Tseng, C.T. Tsai, and T.F. Wu, "Interleaved buck converters with a single-capacitor turn-off snubber," *IEEE Trans. Aerosp. Electron. Syst.* Vol.40, pp.954–967, 2004.
- [11] C. Munoz, "Study of a New Passive Lossless Turn-Off Snubber," In *Proceedings of the International Power Electronics Congress*, pp.147-152, Seoul-Korea, 26–31 October 1998.
- [12] D. Garinto, "A Novel Multiphase Multi-Interleaving Buck Converters for Future Microprocessors," *12<sup>th</sup> International Power Electronics and Motion Control Conference, PEMC 2006*, pp.82-87, Aug-sep 2006.
- [13] A. Joseph, and J. Francis, "Design and Simulation of Two Phase Interleaved Buck Converter," *International Journal of Advanced Research in Electrical, Electronics and Instrumentation Engineering*, vol.4, Special Issue 1, 2015.
- [14] F. Karık, I. Iskender, A. Karaarslan, and N. Genç, "Sarmaşık Yapılı Tek-Faz Doğrultucunun Farklı Akım Kontrol Yöntemleriyle Performans Analizi," *Journal of the Faculty of Engineering and Architecture of Gazi University*, vol.29, no.3, pp.443-450, 2014.
- [15] K. Kayışlı, S. Tuncer, and M. Poyraz, "Kayma Mod Denetleyici Kullanılarak Aktif Güç Faktörü Düzeltimi," *Pamukkale Üniversitesi Mühendislik Bilimleri Dergisi*, vol.14, no.3, pp.253-260, 2008.